Numerical Investigation of Ignition Delay in Methane-Air Mixtures using Conditional Moment Closure

Ahmad S. El Sayed, Cécile B. Devaud

Department of Mechanical and Mechatronics Engineering, University of Waterloo
200 University Avenue West, Waterloo, Ontario, N2L3G1, Canada

1 Introduction

Over the past few years natural gas has been seen as a good alternative fuel for compression ignition engines due to its lower emissions compared to traditional gasolines and its availability world-wide. In order to maintain high engine efficiency, the ignition delay, i.e. the time required for the fuel-air mixture to ignite, needs to be investigated. Due to the difficulties and high costs associated with experimental studies, it is crucial to develop reliable and accurate models to predict autoignition in conditions relevant to engine operation.

The objective of the current study is to develop Conditional Moment Closure (CMC) methods including detailed chemistry suitable to the prediction of autoignition delay of high-pressure methane-air mixtures over a wide range of temperatures. As a first step, first order CMC is implemented and the results are compared with the experimental measurements of Sullivan et al.[1]. The experiments were conducted in a shock tube where high-pressure (75 bar) pure methane at 300 K was injected for 1.5 ms through a 1.1 mm nozzle into the test section filled with air at 30 bar. The ignition delay was determined for air temperatures ranging from 1150 to 1400 K.

2 Computational details

The axisymmetric computational domain has dimensions of 0.15 m (length) $\times$ 0.029 m (radius) and represents one half of the experimental shock tube test section due to symmetry. ANSYS CFX [2] is used to perform the turbulent velocity and mixing field calculations based on an unstructured computational mesh (481 $\times$ 103 unevenly-spaced nodes in the axial and radial directions, respectively). Following the experimental conditions [1], a fixed mass flow rate of 4.875×10^{-3} kg/s and a temperature of 300 K are set at the methane inlet. Experiments also indicated that the flow entering the shock tube test section was subsonic implying that the methane jet should have a high static pressure based on a polytropic gas expansion [3]. In the present simulations, it was not possible to specify both the mass flow rate and the pressure simultaneously at the inlet. Thus, the methane inlet pressure is set to the initial air pressure in the shock tube. This approximation is reasonable for most parts of the flowfield since large pressure gradients are expected to occur only very close to the fuel inlet. The computational domain is initialized with pure air at a given temperature between 1200 K to 1400 K and at a static pressure of 30 bar. In the absence of experimental data, the predicted transient jet penetration length is compared with the correlation developed by Hill et al.[4]. Best agreement (within 5%) is achieved using a modified k-ε turbulence model with $C_{\varepsilon 1}$ adjusted to 1.535. This value is kept throughout the simulations and an adaptive time step is used.

Turbulent combustion is modelled using Conditional Moment Closure (CMC) [5]. For simplicity, the

Correspondence to : cdevaud@mecheng1.uwaterloo.ca

turbulent flowfield using CFX and CMC calculations are decoupled, i.e. the turbulent flowfield is used as an input to the CMC routine. This is a reasonable approximation since the temperature difference is very small until ignition is reached. A similar procedure was successfully applied to autoignition by Markides et al.[6] . As a first step, first order closure for the chemical source term is considered. The effect of conditional fluctuations on autoignition for the present conditions will be investigated in future work. In CMC the species mass fractions, as well as enthalpy or temperature, are conditionally averaged on mixture fraction in the case of turbulent non-premixed combustion. Thus, the transport equations for the conditional scalars need to be solved in physical and mixture fraction spaces. In the present study, the CMC equations are cross-stream averaged on the basis of small radial dependence of the conditional species mass fractions in a jet [7]. The resulting transport equation for each conditional species mass fraction, Q_α, is:

$$\underbrace{\frac{\partial Q_\alpha}{\partial t}}_{\text{transient term}} = \underbrace{-\left[\{\langle u_x|\eta\rangle\}_{R^+} - \left\{\frac{D_t}{\tilde{P}(\eta)}\frac{\partial \tilde{P}(\eta)}{\partial x}\right\}_{R+} - \left\{\frac{\partial D_t}{\partial x}\right\}_{R^+}\right]\frac{\partial Q_\alpha}{\partial x} + \{D_t\}_{R^+}\frac{\partial^2 Q_\alpha}{\partial x^2}}_{\text{spatial transport}} + \underbrace{\frac{1}{2}\{\langle\chi|\eta\rangle\}_{R^+}\frac{\partial^2 Q_\alpha}{\partial \eta^2}}_{\text{micro-mixing}} + \underbrace{\frac{\langle\dot{\omega}_\alpha|\eta\rangle}{\langle\rho|\eta\rangle}}_{\text{chemical source}} \quad , \tag{1}$$

where x is the axial distance from the entrance of the shock tube, η a mixture fraction value, $\langle u_x|\eta\rangle$ the conditional axial velocity, $D_t = (C_\mu/Sc_t)(k^2/\varepsilon)$ the turbulent diffusivity with the constant C_μ equal to 0.09, the turbulent Schmidt number Sc_t set to 0.9, k is the turbulent kinetic energy and ε the dissipation rate of the turbulent kinetic energy, $\tilde{P}(\eta)$ is the Favre-averaged Probability Density Function (PDF), $\langle\chi|\eta\rangle$ represents the conditional mean scalar dissipation rate, $\langle\dot{\omega}_\alpha|\eta\rangle$ corresponds to the conditional chemical source term and $\langle\rho|\eta\rangle$ is the conditional density. Gradient diffusion for the turbulent flux, high Reynolds number and no differential diffusion are assumed in the derivation of Eq.(1). $\{F(r)\}_R$ and $\{F(r)\}_{R^+}$ denote the area-weighted and the cross-stream averages of the scalar $F(r)$, respectively. The latter is defined as $\{F(r)\}_{R^+} = \{F(r)\tilde{P}(\eta)\}_R/\{\tilde{P}(\eta)\}_R = \int_0^R F(r)\tilde{P}(\eta)rdr/\int_0^R \tilde{P}(\eta)rdr$ where R is a large radius determined according to a cutoff value of 10^{-2} for the Favre-averaged mixture fraction in the flowfield calculations. Smaller cutoff values were tested and the differences in the cross-stream averages were shown negligible. Two different expressions are implemented for the conditional scalar dissipation rate: Girimaji's model [8] and the Amplitude Mapping Closure (AMC) [9]. The linear model is used for the conditional velocity [5]. Detailed chemistry for methane combustion is included using the chemical mechanism developed by Huang et al.[3] consisting of 38 species and 192 steps. For consistency with the CFX calculations, no pressure work is included in the CMC calculations. Consequently, the conditional temperature is calculated from the conserved conditional enthalpy and species concentrations. The mesh consists of 63 nodes in mixture fraction space refined around stoichiometry ($\eta = 0.055$) and 28 unevenly spaced grid points in the axial direction covering two thirds of the CFX domain length. Finite differences and a fractional step method, previously used by Devaud et al.[10], are applied to solve Eq.(1) for each species. Turbulent mixing field parameters are updated every 50 μs in the CMC calculations. The ignition criterion is based on a 75 K increase in the conditional temperature at any point in the domain. The results were shown to be grid independent.

3 Results and Discussion

In order to investigate the role of spatial transport in the ignition mechanism, two series of simulations are performed. First, spatial transport is not included, i.e., only the transient term, micro-mixing and the chemical source are kept. In the second series, all the terms in Eq.(1) are considered. In both cases the two mixing models are implemented. The predicted ignition delays are compared with

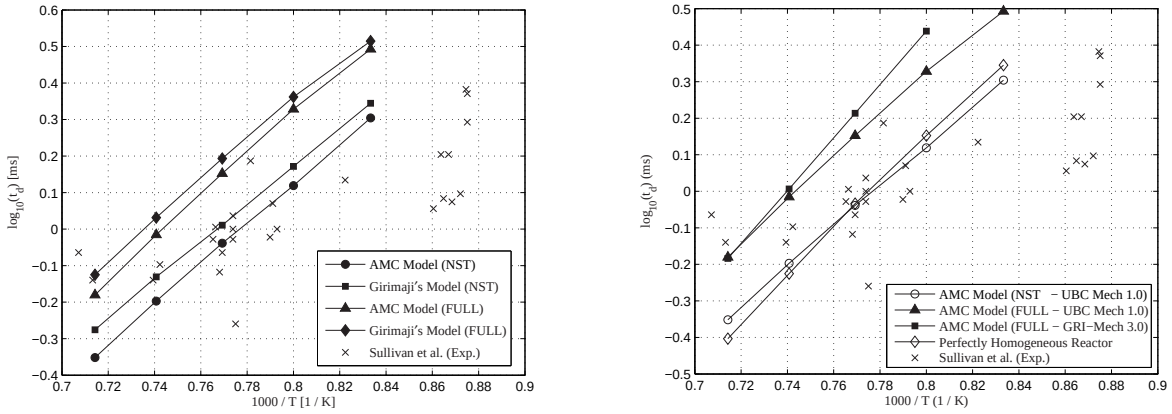

(a) (b)

Figure 1: Ignition Delay for different air temperatures, Full: Eq.(1), NST: No Spatial Transport.

Table 1: x_{ign} (cm), η_{ign}, t_d (ms) and $\{\langle\chi|\eta\rangle\}_{R^+,ign}$ (s^{-1}) using the AMC model for $\langle\chi|\eta\rangle$.

	NST				Full (Eq.(1))			
T_{air} (K)	x_{ign}	η_{ign}	t_d	$\{\langle\chi|\eta\rangle\}_{R^+,ign}$	x_{ign}	η_{ign}	t_d	$\{\langle\chi|\eta\rangle\}_{R^+,ign}$
1200	4.00	0.02475	2.015	1.54	5.00	0.02200	3.11	0.27
1250	3.75	0.02475	1.315	2.32	4.50	0.02200	2.13	1.01
1300	3.50	0.02200	0.915	2.61	4.00	0.01925	1.42	1.29
1350	2.75	0.01650	0.635	3.04	3.25	0.01650	0.97	1.77
1400	2.25	0.01650	0.445	5.95	2.75	0.01650	0.66	2.94

the experimental data of Sullivan et al.[1] in Fig.1. As can be seen in Fig.1 a) the results show very good agreement with the experimental data and the trend of increasing ignition delay for decreasing air temperature is well reproduced. Both scalar dissipation models yield comparable values with the AMC model predicting ignition slightly earlier. It can be seen that the ignition location (x_{ign}) increases with decreasing air temperature and remains above 20 (nozzle) diameters away from the fuel inlet. In contrast, the conditional scalar dissipation at ignition decreases with decreasing air temperature. This is explained by the fact that chemical activity is larger at higher temperatures and can compete with more intense turbulent mixing, thus ignition occurs earlier. In all cases, ignition always occurs in fuel-lean mixtures (around 0.02) and at low scalar dissipation rates in conditional space. Comparison of the results from the two series clearly indicates that spatial transport increases ignition delay. Figure 1b) presents the predicted ignition delays using two different chemical mechanisms, UBCMech 1.0 [3] and GRI 3.0 [12] using the AMC model for the conditional scalar dissipation compared with homogeneous reactor simulations performed at η_{ign} and CMC calculations without spatial transport for different air temperatures. The results including the GRI mechanism are very close to those with the UBC kinetics for air temperatures greater than 1300K (within 5%). At lower air temperatures, some differences appear. For example, GRI 3.0 overpredicts the UBCMech ignition delay by 29% for a value of air temperature equal to 1250 K. Both mechanisms include a large number of species and steps. However, UBCMech has been optimized for low air temperatures and high pressures [3]. Thus, it is expected to perform better in the present autoignition conditions. As shown in Fig.1b) the homogeneous reactor values are lower

than those predicted with the full CMC calculations but very close to the NST (No Spatial Transport) results. This is an expected behaviour since the homogeneous reactor includes the composition at one η value selected to be η_{ign} and no spatial transport is considered.
Table 1 provides further details on the location of ignition in the axial direction (x_{ign}) and in mixture fraction space (η_{ign}), the ignition delay (t_d) and the value of $\{\langle\chi|\eta\rangle\}_{R^+}$ at the ignition point $\left(\{\langle\chi|\eta\rangle\}_{R^+,ign}\right)$. As can be seen, spatial transport increases the axial location where ignition occurs and the scalar dissipation at the ignition point is much lower than the value obtained in the calculations in the absence axial transport. For both series, the ignition location in mixture fraction space remains approximately the same. Wright et al.[11] also noted the significant role of spatial transport in their calculations but observed an opposite effect on the ignition delay. This difference may be explained by the fact that different operating and boundary conditions were used in their simulations. As shown in Fig.2, the critical χ_0 value above which ignition cannot occur is around 400 s^{-1} resulting in a value for $\langle\chi|\eta\rangle$ of approximately 10 s^{-1} for $T_{air} = 1300$ K. The scalar dissipation values at ignition in Table 1 are much smaller (2.61 s^{-1} for NST and 1.29 s^{-1} for full CMC calculations).

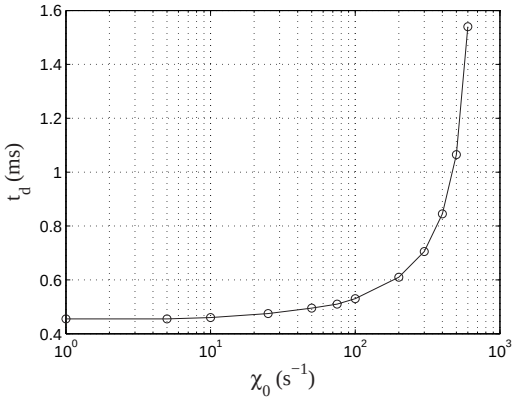

Figure 2: Flamelet calculation with T_{air} (air temperature) = 1300K and AMC using $\langle\chi|\eta\rangle = \chi_0\ G(\eta)$ with $G(\eta) = \exp(-2\text{erf}^{-1}(2\eta - 1)^2)$ [9].

Figure 3 presents the change in the major conditional species concentrations relative to their initial values. As expected, the conditional concentrations of the reactants CH_4 and O_2 have decreased while H_2O, CO_2, CH_2O, C_2H_6, C_2H_4 and CO concentrations have gone up. The low CO_2 concentration compared to the relatively higher CO radical concentration is explained by the fact that CO_2 production occurs through the oxidation of CO by OH, HO_2, O_2 and O, but those reactions are inhibited by the presence of CH_4. Furthermore, a complete oxidization requires a substantial rise in temperature. At the ignition time, the temperature rise is equal to 75 K at most which is insufficient for the complete oxidization. Although the CMC equations are cross-stream averaged and solved in one dimension it is possible to obtain the Favre averaged temperatures in two dimensions (x, r) using Eq.(2):

$$\tilde{T}(x,r) = \int_0^1 \{\langle T(x,\xi)|\xi = \eta\rangle\}_{R^+} \tilde{P}(x,r,\eta)\ d\eta, \tag{2}$$

where the Favre-averaged temperature, $\tilde{T}$ is calculated by integrating the product of the conditional temperature and PDF over mixture fraction space. The temporal variation of the Favre-averaged temperatures relative the initial temperatures in the spatial domain at $x = 3.75$ cm (x_{ign}) is shown in Fig.4a). As expected, the Favre-averaged temperatures rise with increasing time and the peak of temperatures slightly moves to larger radial distances with time following the position of the jet shear layer. Until now, the ignition criterion has been defined on the conditional temperature difference of 75K. Ignition

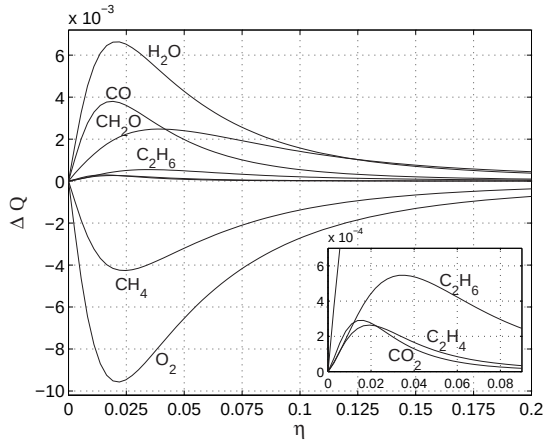

Figure 3: Change in the concentration of the major species at ignition for $T_{\text{air}} = 1300$K and AMC.

could also be determined using the Favre-averaged temperature difference. Thus the ignition location in physical space can be determined. Figure 4b) presents the mixture fraction contours at ignition for a value of air temperature equal to 1300 K. It can be seen that the ignition point is located at an axial distance equal to 3.75 cm and a radial distance of approximately 0.51 cm. This is situated in the shear layer of the jet close to the stoichiometric value of mixture fraction equal to 0.055. The new ignition delay based on the Favre-averaged temperatures is found to be 1.44 ms compared to 1.42 ms based on the conditional temperatures for an air temperature of 1300K. Thus, the ignition criterion based on conditional or Favre-averaged temperatures provides comparable values of ignition delay.

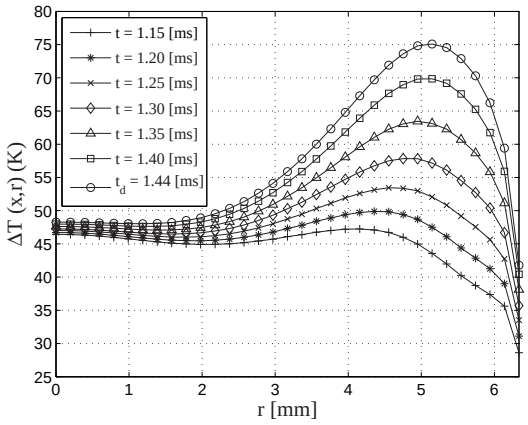

(a) Favre-averaged temperature change at ignition time.

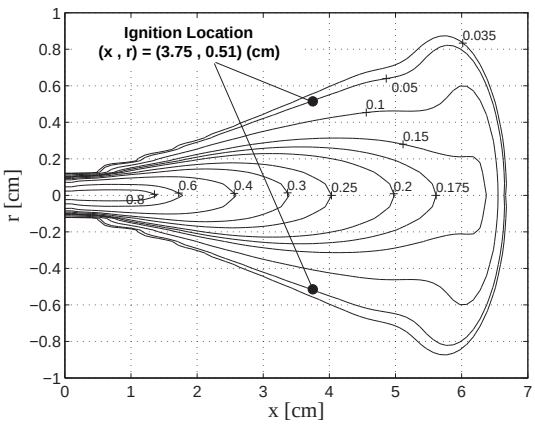

(b) Ignition locations superimposed on mean mixture fraction contours.

Figure 4: Favre-averaged results for $T_{\text{air}} = 1300$K and AMC model.

4 Conclusions

Our results for ignition delay using first order CMC are in very good agreement with the experimental measurements [1] and are consistent with previous autoignition simulations [6, 11, 13]. The trend of decreasing ignition delay with increasing air temperature was very well reproduced. The present results also showed that spacial transport delays ignition and that the two mixing models yield comparable results with the AMC model producing slightly shorter delays. It was found that both spatial transport and micro-mixing in mixture fraction space were important in the modelling of autoignition. Two chemical mechanisms were tested: UBCmech 1.0 and GRI 3.0. At lower temperatures, the GRI kinetics produced larger ignition delays.
Other aspects will be considered such as testing different ignition criteria and non-homogeneous mixing models and performing CMC calculations in two spatial dimensions (fully coupled with the CFD calculations). Further development related to the inclusion of the conditional fluctuations will be investigated.

Acknowledgement

Financial support from AUTO 21 is gratefully acknowledged.

References

[1] Sullivan GD, Huang J, Wang T, Bushe WK, Rogak S (2005). Emissions variability in gaseous fuel direct injection compression ignition combustion. SAE 2005-01-0917.

[2] Ansys CFX 10.0 (2006).

[3] Huang J, Hill PG, Bushe WK, Munshi SR (2004). Shock-tube study of methane ignition under engine-relevant conditions: experiments and modeling, Combust. Flame 136:25.

[4] Hill PG, Ouellette P (1999). Transient turbulent gaseous fuel jets for diesel engines. J. Fluid. Mech 121:93.

[5] Klimenko AYu, Bilger RW (1999). Conditional moment closure for turbulent combustion. Prog. Energy Combust. Sci. 25:595.

[6] Markides CN, De Paola G, Mastorakos E (2006) Measurements and simulations of mixing and autoignition of an n-heptane plume in a turbulent flow of heated air. Exp. Therm. Fluid Sci. (In Press).

[7] Klimenko AYu (1995). Note on the conditional moment closure in turbulent shear flows. Phys. Fluids 7(2):446.

[8] Girimaji S (1992). On the modeling of scalar diffusion in isotropic flows. Phys. Fluids A 4(11): 2529.

[9] O'Brien EE, Jiang TL (1991). The conditional dissipation rate of an initially binary scalar in homogeneous turbulence. Phys. Fluids A 3(12):3121.

[10] Devaud CB, Bray KNC (2003). Assessment of the applicability of conditional moment closure to a lifted turbulent flame: first order closure. Combust. Flame 132:103.

[11] Wright YM, De Paola G, Boulouchos K, Mastorakos E (2005). Simulations of spray autoignition and flame establishment with two-dimensional CMC. Combust. Flame 143:402

[12] Smith G., Golden D., Frenklach M., Moriarty N., Eiteneer B., Goldenberg M., Bowman T., Hanson R., Song S., Gardiner W., Lissianski V., Qin Z, `http://www.me.berkeley.edu/gri_mech/`

[13] Kim S., Huh K.Y., and Frazer R.A., Proc. of the Combust. Institute 28:185 (2000).